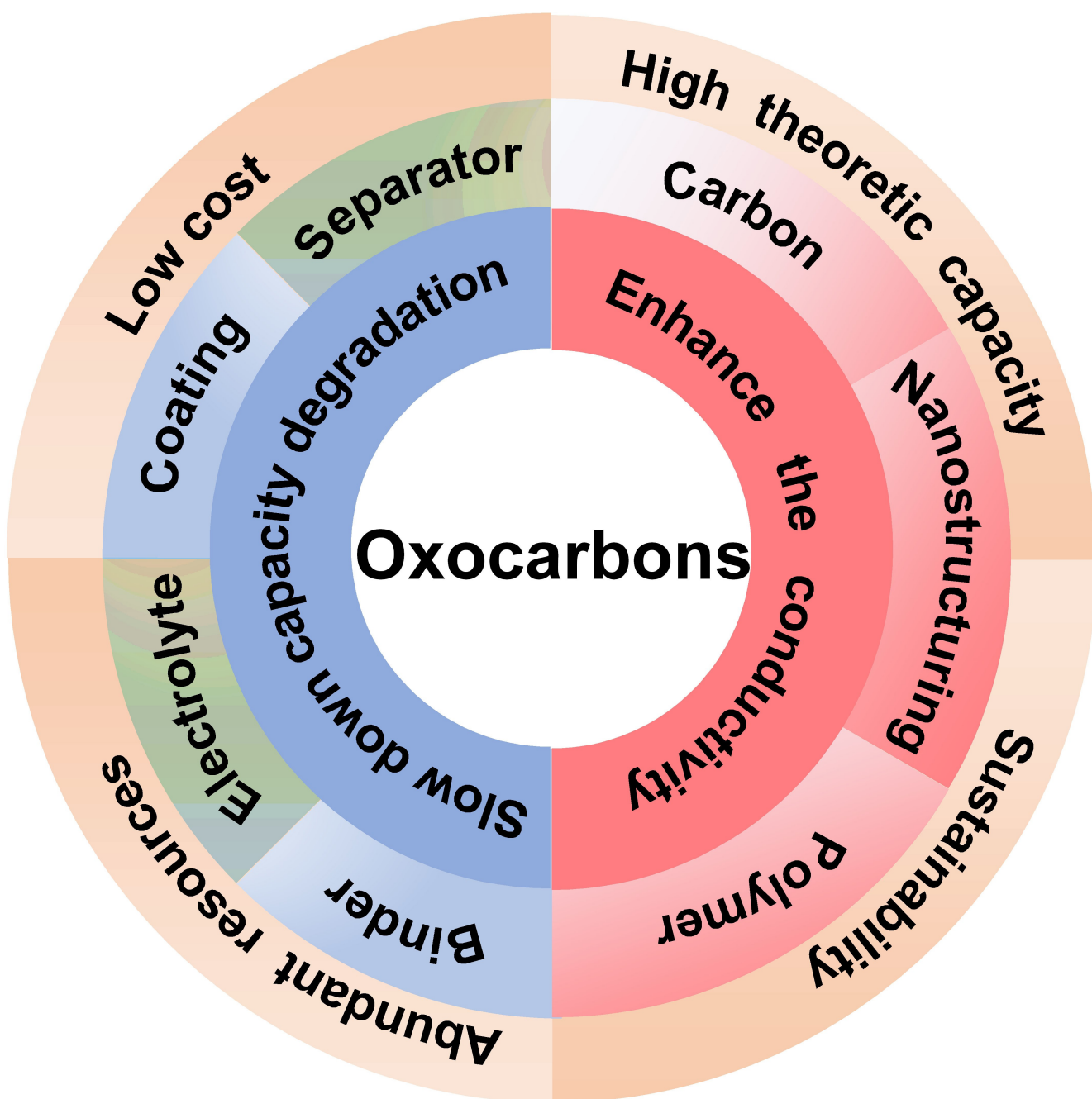


VIP Very Important Paper

Oxocarbons Electrode Materials for Alkali Ion Batteries: Challenges, Strategies and Development

Zhengna Zhang,^[a] Jianjun Ma,^[b] Rui Zhang,^[a] Ranjusha Rajagopalan,*^[a] Yougen Tang,*^[a] Yu Ren,^[c] and Haiyan Wang*^[a]



Benefiting from the high theoretic capacity, structural designability, low cost, abundant resources and sustainability, oxocarbons materials have attracted extensive attention as a promising candidate to replace inorganic electrode materials for alkali ion batteries (AIBs). This review focuses on the in-depth evaluation of the electrochemical properties of oxocarbons for lithium, sodium and potassium ion batteries. Further, we summarize the evolution, challenges and opportunities of oxocarbon compounds based on our current understanding. In

addition, we identified two main aspects that limit their applications as electrode materials: 1) inferior conductivity and 2) fast capacity decay. Hence, in this review we also integrate different strategies to improve these two aspects, e.g., compositing with carbon, grafting conductive polymers, nanostructuring, optimizing electrolytes, designing interface, and selecting appropriate binders. This review can be useful to understand the practical application and commercial feasibility of such materials for different AIBs applications.

1. Introduction

Energy, as an important aspect of the modern economy, has become an essential foundation for the survival/development of human society and plays a significant role in promoting economical/social development. In the era of industrialization, due to a large amount of fossil fuel consumption, energy crisis and serious environmental pollution had evolved which lead to the realization of the importance of investigation and development of clean and efficient energy storage systems (ESSs).^[1] Because of its high energy density, long life, and good safety performance, alkali ion batteries have become the most promising ESSs.^[2] Since the first successful commercialization in 1991^[3] with transition metal oxides as a cathode, carbon as an anode, and LiPF₆ dissolved in carbonate as an electrolyte, lithium ion batteries (LIBs) became the world leader among different ESSs. In the past few decades, research on cathode materials for ESSs mainly focuses on inorganic electrode materials (such as layered transition metal oxides,^[4] polyanionic-based materials,^[5] Prussian blue analogues,^[6] etc.), most of which are derived from ores and exhibit ideal electrochemical properties.^[7] However, with the increasing popularity of new electric vehicles and the rapid development of the energy storage market, the demand for ESSs has risen which drives the researchers to explore different electrode and electrolyte materials.^[8] Thus, scientists across the globe are trying to develop new types of alkali ion batteries (AIBs).^[9] The elements Na and K have similar physicochemical properties of Li but have lower cost and abundant resources (Li: 0.0017%, Na: 2.36% and K: 2.09% in the earth's crust).^[10] This leads the researchers to focus more on sodium ion batteries (SIBs) and

potassium ion batteries (PIBs) in recent years.^[11] At present, the main drawback of SIBs and PIBs is the structural damage during the Na⁺ and K⁺ deintercalation process because of the large ionic radius.^[12] Hence, host materials such as organic compounds that are capable of tolerating large sized ion deintercalation have attracted considerable attention.^[13]

Organic electrode materials are highly likely to replace inorganic materials due to their superior properties.^[14] 1) Organic materials are mainly composed of C, H, O, N elements, showing non-toxic, environmentally friendly, low-cost, renewable, and sustainable characteristics.^[14b] 2) It is widely distributed in the animals and plants on the earth and can be synthesized/obtained from biomass.^[15] 3) Functional molecular structures can be designed, hence we can prepare the material according to the applications.^[8a] 4) The theoretical capacities of some organic compounds such as cyclohexanehexone (957 mAh g⁻¹) are much higher than those of inorganic compounds.^[16] Recently, a large number of studies have started focusing on organic electrode compounds based on C=O (carbonyl) reaction, C=N reactions and doping reactions.^[13a,16,17]

Oxocarbons belong to the category of carbonyl compounds and contain multiple carbonyl groups, which act as redox-active sites for AIBs. The oxocarbon compounds exhibit high theoretical capacity and low solubility when they are employed as electrode materials.^[18] For instance, Chen *et al.* prepared lithiated oxocarbon salt (Li₂C₆O₆), via low-cost processing technique, which showed a high reversible capacity of 580 mAh g⁻¹.^[15a] In this work, they proposed that the capacity decay was directly related to the material's dissolution in the electrolyte. Another research group proposed that the capacity decay of Na₂C₆O₆ cathode material for SIBs was resulted from irreversible phase change during the reaction.^[19] For this material, a reversible capacity of 484 mAh g⁻¹ (theoretical capacity: 501 mAh g⁻¹) was achieved by properly regulating the electrolyte conditions and the particle size of the active material.^[19] Chen and co-workers have prepared M₂(CO)_n (M can be Li, Na, K; n=4, 5, 6) and have reported that when n=4, the material showed difficulty in accepting metal cations. However, M₂(CO)₅ and M₂(CO)₆ compounds could show ultrafast and reversible cation deintercalation in an appropriate voltage range. Moreover, the first rocking-chair PIBs was constructed with K₂C₆O₆ as positive and K₄C₆O₆ as negative electrode, although exhibiting a plateau voltage of 1.1 V and an energy density of 35 Wh kg⁻¹, which laid a solid foundation for the fabrication of more high renewability and wide abundance

[a] Z. Zhang, R. Zhang, Dr. R. Rajagopalan, Prof. Y. Tang, Prof. H. Wang
 Hunan Provincial Key Laboratory of Chemical Power Sources
 College of Chemistry and Chemical Engineering
 Central South University
 Changsha, 410083, China
 E-mail: rranjusha@gmail.com
 ygtang@csu.edu.cn
 wanghy419@csu.edu.cn

[b] Prof. J. Ma
 Material Corrosion and Protection Key Laboratory of Sichuan Province
 Sichuan University of Science & Engineering
 Zigong 643000, China

[c] Prof. Y. Ren
 TEC Materials Development Team
 Tianmu Lake Institute of Advanced Energy Storage Technologies
 Changzhou 213300, China

AlBs.^[18] In addition, proper mixing of organic and inorganic materials is also an effective strategy to restrict the dissolution of active materials.^[20] For instance, a three-dimensional (3D) sandwich structure of Na₄C₆O₆-graphene-Na₄C₆O₆ was obtained by combining organic-inorganic tetrahydroxybenzoquinone (Na₄C₆O₆) and graphene via a simple hydrothermal method. This unique porous structure not only improved the conductivity of the Na₄C₆O₆ but also provided a pathway for fast ion transport. Thus, a high reversible capacity of 885 mAh g⁻¹ (first discharge capacity) with fast charging was achieved.^[20] Although many such strategies have been widely used to enhance the properties of oxocarbon compounds as electrode materials for AlBs, more in-depth research are still required.

Our literature review on oxocarbon compounds for AlBs has shown that there are many reports available for the electrochemical performance evaluation. However, to the best of our knowledge, there is not a single review which consolidates different explored oxocarbon compounds for different AlBs. Hence, the motivation behind this review is to amalgamate the electrochemical properties of various oxocarbons investigated for different AlBs. In this aspect, the present review focuses on the comprehensive analysis of different oxocarbon materials, its electrochemical performances, evolution, challenges and opportunities. The advantages and strategies of oxocarbon based electrodes in AlBs were summarized in Figure 1. We believe that this review can provide deep insights into the development of environmentally friendly, cost-effective, high performing rechargeable battery for the future.

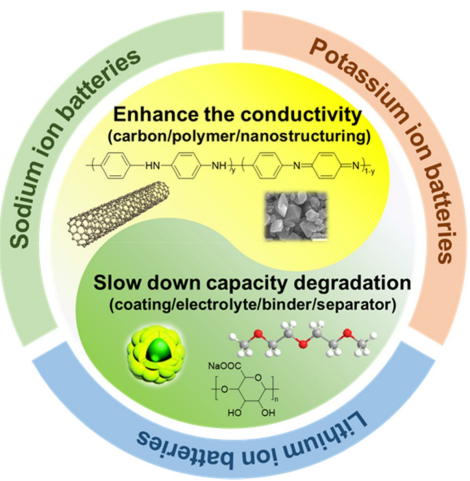


Figure 1. Schematic illustration of advantages and strategies to improve the electrochemical performance of oxocarbon based electrodes in different AlBs.

2. Evolution

Investigation on oxocarbon based compounds has started about six decades back. Figure 2 illustrates the evolution of oxocarbon compounds. In 1958, Cohen *et al.*, reported a novel anion (C₄O₄²⁻) which was considered as the first explored oxocarbon based compound.^[21] Later, an increasing number of oxocarbon based compounds with multiple carbonyl groups were introduced.^[18,22] In recent years, carbonyl groups have been regarded as one of the redox active centers for electrode materials.^[18,23] In 2008, Chen *et al.* prepared dilithium rhodizo-



Zhengna Zhang received her Bachelor's degree in Materials Science and Engineering at Northwest Normal University in 2019. She is pursuing a Master's degree in College of Chemistry and Chemical Engineering, Central South University. Her current research interests focus on high-performance organic Na⁺/K⁺ batteries based on structure design and modification of oxocarbon compounds.



Ranjusha Rajagopalan received her Ph.D in Physics with specialization in battery technology from University of Wollongong, Australia in the year 2017. She is currently working on functionalized organic/inorganic materials for developing high performance metal ion batteries, including sodium and potassium ion batteries at College of Chemistry and Chemical Engineering, Central South University, China.



Yougen Tang earned his Ph.D in Material science at Central South University. From 2000, he is a Professor in College of Chemistry and Chemical Engineering at Central South University. He is the director of Institute of Chemical Powder Sources and Materials at Central South University and he is also the head of Hunan Provincial Key Laboratory of Chemical Power Sources. He has published over 200 refereed papers. His current research interests are focused on the new energy materials and advanced batteries.



Haiyan Wang earned his Ph.D degree (2012) in Applied Chemistry at Central South University. He once studied at University of St. Andrews as a visiting Ph.D student under supervision of Prof. Peter G. Bruce. Starting in 2016, He worked for 2 years at the Hong Kong University of Science and Technology as a Hong Kong Scholar. Now he is a Professor in College of Chemistry and Chemical Engineering at Central South University. His current research interests mainly focused on the new energy materials and advanced batteries. He has published over 120 refereed papers as the first or corresponding author (total citations Eover 5500 times and h-index 45).

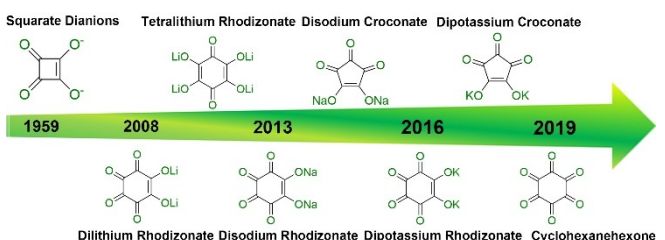


Figure 2. Timeline of the development of oxocarbon compounds.

nate ($\text{Li}_2\text{C}_6\text{O}_6$) and used as a cathode material for LIBs which exhibited a high reversible capacity of 580 mAh g^{-1} during the first discharge. The investigation on $\text{Li}_2\text{C}_6\text{O}_6$ showed that each molecular unit could participate in reversible insertion/extraction process with four lithium ions.^[15a] This study opened up the door for oxocarbon based electrode materials to fabricate green and sustainable batteries. The precursor myo-inositol is widely distributed in plant seeds and germ (such as soybean, peanut).^[24] In 2009, Chen *et al.* prepared tetralithium salt of tetrahydroxybenzoquinone ($\text{Li}_4\text{C}_6\text{O}_6$) using different methods and assembled first all-organic battery which showed good electrochemical performance.^[25] Besides oxocarbon salts of lithium, other kinds of oxocarbon salts have been reported in successions, such as $\text{Na}_2\text{C}_6\text{O}_6$, $\text{K}_2\text{C}_6\text{O}_6$ for SIBs and PIBs applications, respectively.^[17,26] However, those materials possess poor cycling stability and dissolution issue. Thus, later studies focused on overcoming these problems. In 2013, Chihara *et al.* reported the cathode properties of $\text{Na}_2\text{C}_6\text{O}_6$ for SIBs. This study proved that the oxocarbon material was suitable for Na^+ intercalation/deintercalation process and showed outstanding electrochemical performance without the addition of conductive carbon. $\text{Na}_2\text{C}_6\text{O}_6$ showed a reversible capacity of $\sim 270 \text{ mAh g}^{-1}$ and an energy density of $\sim 370 \text{ Wh kg}^{-1}$ ^[17b], which are comparable/superior to the traditional inorganic materials. In 2014, a research group synthesized $\text{Na}_2\text{C}_5\text{O}_5$ nanowires with different diameters. These nanowires could effectively enhance the electronic conductivity and kinetics of oxocarbon salts when employed as an electrode in LIBs.^[27] In 2016, a research team explored $\text{K}_2\text{C}_6\text{O}_6$ and $\text{K}_2\text{C}_5\text{O}_5$ as host materials for ultrafast charge/discharge for PIBs. When applied as K^+ insertion/extraction electrode, the $\text{K}_2\text{C}_6\text{O}_6$ could demonstrate a capacity of 212 mAh g^{-1} at 0.2 C and retained 164 mAh g^{-1} at 10 C .^[18] In 2017, great progress has been made in using $\text{Na}_2\text{C}_6\text{O}_6$ as positive electrode for SIBs.^[19] A research group revealed that the phase transformation of $\text{Na}_2\text{C}_6\text{O}_6$ during cycling was the reason for the lower experimental capacity as compared to the theoretical value of 501 mAh g^{-1} .^[19] In 2019, Chen *et al.* successfully fabricated cyclohexanehexone (C_6O_6) and applied for lithium storage. It delivered an ultrahigh capacity of 902 mAh g^{-1} with an average voltage of 1.7 V at 20 mA g^{-1} , which is corresponding to the energy density of 1533 Wh kg^{-1} .^[16]

3. Molecular Structure and Properties

The two main categories of oxocarbons are 1) cyclic oxocarbon acid ($\text{H}_n\text{C}_n\text{O}_n$, $n=3, 4, 5, 6$) and 2) oxocarbon salts ($\text{M}_x\text{C}_n\text{O}_n$, $\text{M}=\text{Li}, \text{Na}, \text{K}$ etc. alkali metal; and NH_4^+ complex cation: $x=2, 4$; $n=3-6$).^[28,29] The structure of the material determines its physicochemical properties and performance. Understanding of the material structure is an important aspect to design high-performance electrode for storage applications. In general, oxocarbon compounds are made up of cations (H^+ , Li^+ , Na^+ , K^+ etc.) and planer cyclic dianions ($\text{C}_n\text{O}_n^{2-}$, $n=4-6$).^[30] These dianions possess a series of symmetric resonant stable anions where its salts are aromatic in nature.^[31] Typically, $\text{Na}_2\text{C}_6\text{O}_6$ compound consists of alternating $\text{C}_6\text{O}_6^{2-}$ anion layer and hexagonally packed Na cation layer. Its space group is Fddd (Figure 3).^[19,32] The sodium-oxygen ionic bond in this compound is stable in organic solvents, thus effectively avoids its dissolution in carbonate and ether-like electrolytes.^[19] These compounds can be easily obtained from biomass and have the advantages of high theoretical capacity,^[15a,19] outstanding electrochemical performance,^[33] thermal stability^[14b] and so on. Among these categories, many research studies have focused on secondary battery electrodes based on alkali salt of cyclic oxocarbons.^[17b,18,26a,34] It is worth noting that Otaegui and Marinoco's group used $\text{Na}_2\text{C}_4\text{O}_4$ and $\text{Na}_2\text{C}_6\text{O}_6$ as sacrificial templates to overcome sodium deficiency issues in P2-phase $\text{Na}_{0.67}\text{Fe}_{0.5}\text{Mn}_{0.5}\text{O}_2$ and $\text{Na}_{0.67}\text{Mn}_{0.6}\text{Fe}_{0.25}\text{Co}_{0.15}\text{O}_2$ compounds, resulting in high energy density and good cycle stability in full-cell format.^[35]

4. Oxocarbon Based Compounds for LIBs

The development of oxocarbon based materials has brought hope to achieve low-cost, environmental benignity, and highly safe LIBs.^[16,25,27,36] The oxocarbon based compounds have shown inherently high solubility and low conductivity in LIBs. Hence, the actual capacity of this kind of material is quite different from the theoretical capacity, and it shows fast capacity decay upon cycling.^[36,37] In addition, the formation of unstable SEI film and its dissolution in electrolytes will also cause rapid capacity decay.^[38] To address these issues, researchers have proposed various strategies such as morphology control, interface

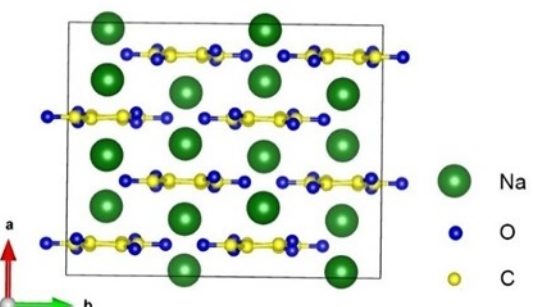


Figure 3. Crystal structure of $\text{Na}_2\text{C}_6\text{O}_6$.

engineering and structure regulating.^[36,37] It should be noted that the research on this category of material is still in its preliminary stage, hence we believe that there are plenty of opportunities for the further enhancement of the performance of this material for practical LIBs applications.

4.1. Cathode Materials

To be used in practical battery applications, electrode materials must meet some strict requirements.^[13a] High power density, superior energy density, excellent cycle performance, low cost, sustainability and good safety factor have always been the pursuit of energy storage materials.^[13a,39] The carbonyl organic salt of Li ($\text{Li}_x\text{C}_6\text{O}_6$) was first used in LIBs, which has a milestone for the development of oxocarbon based materials in the field of energy storage.^[15a] The precursor, rhodizonate acid ($\text{H}_2\text{C}_6\text{O}_6$), can be obtained directly from myo-inositol which is widely present in plants or corn steep liquor.^[40] A study revealed that $\text{Li}_2\text{C}_6\text{O}_6$ material could provide a high capacity of 580 mAh g⁻¹ and high temperature stability at 220 °C, but the poor cycle life limits its practical applications.^[15a] Hence, capacity attenuation is considered as the fatal weakness of this type of electrode material. To explore the cause of the capacity decay, Kim *et al.* carried out the first-principles calculations.^[41] The results revealed that there was no obvious change during the lithium intercalation process, but while delithiation the electrode particles were crushed and peeled-off from the current collector.^[41] Further, the large surface area accelerated the dissolution of active material into the electrolyte, resulting in capacity attenuation. Moreover, the first-principles calculation results showed that the $\text{C}_6\text{O}_6^{2-}$ layer spacing became larger during the insertion and extraction of lithium, resulting in the peeling-off of the electrode material. Hence, to effectively reduce the attenuation for achieving a lithium secondary battery with excellent chemical properties, the dissolution and the change in crystal structure should be fully addressed.^[41]

Croconic acid disodium salt (CADS, $\text{Na}_2\text{C}_5\text{O}_5$) nanowires have been explored for LIBs. A study reported the superior cycle stability and high rate performance of CADS nanowires as compared to micropillar and microwire structured materials.^[27] Although the conductivity of this CADS nanowire is unsatisfactory, its small size and large specific surface area could effectively enhance the reaction kinetics, thus allowing Li^+ to transport faster within the material. The reaction mechanism obtained through theoretical calculations and inductively coupled plasma (ICP) experiment is provided in Figure 4. In short, 2Li^+ were first inserted into $2\text{C}=\text{O}$ (conjugated with $\text{C}=\text{C}$ structure). Then through the lithium insertion/ion exchange process, the 3,4,5-trioxocyclopentene-1,2-diol dilithium salt ($\text{Li}_2\text{C}_5\text{O}_5$) were formed. Subsequently, during the reversible de/lithiation reaction, $\text{Li}_2\text{C}_5\text{O}_5$ and $\text{Li}_4\text{C}_5\text{O}_5$ could be converted reversibly. The $\text{Na}_2\text{C}_5\text{O}_5$ nanowires prepared by this simple anti-solvent method hardly underwent any crushing and volume expansion during the electrochemical process. In addition, it has shown good contact with conductive carbon black, which

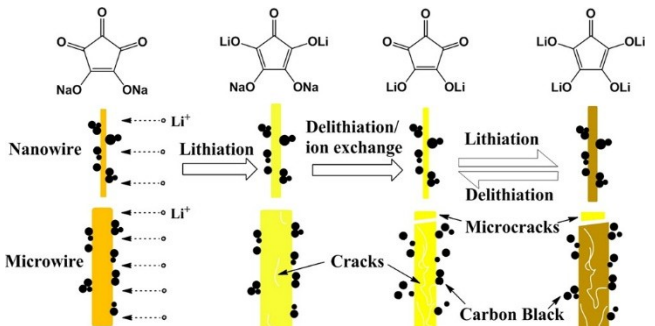


Figure 4. Schematic illustration of lithiation/delithiation mechanism for $\text{Na}_2\text{C}_5\text{O}_5$. Reproduced from Ref. [27] with permission. Copyright (2014), American Chemical Society.

could be the reason for its impressive electrochemical performance.^[27]

A research group adopted multiple strategies, such as interface modification of inorganic materials and coating multiple layers of electrochemically stable FeF_3 on the surface of organic materials, to avoid direct contact between electrolyte and organic materials. Meanwhile, the rGO could improve the electronic conductivity of the electrode systems.^[37] Figure 5(a) illustrates different morphologies of $\text{Li}_2\text{C}_6\text{O}_6$ along with the simulation of morphological change during charge-discharge process. As illustrated in Figure 5(b), three samples show similar charge-discharge curves during the first cycle. Nevertheless, $\text{Li}_2\text{C}_6\text{O}_6$ and $\text{Li}_2\text{C}_6\text{O}_6/\text{rGO}$ suffer from severe capacity attenuation in the following cycles (Figure 5c,d), which resulted from the dissolution of $\text{Li}_2\text{C}_6\text{O}_6$ particles into the electrolyte. During the

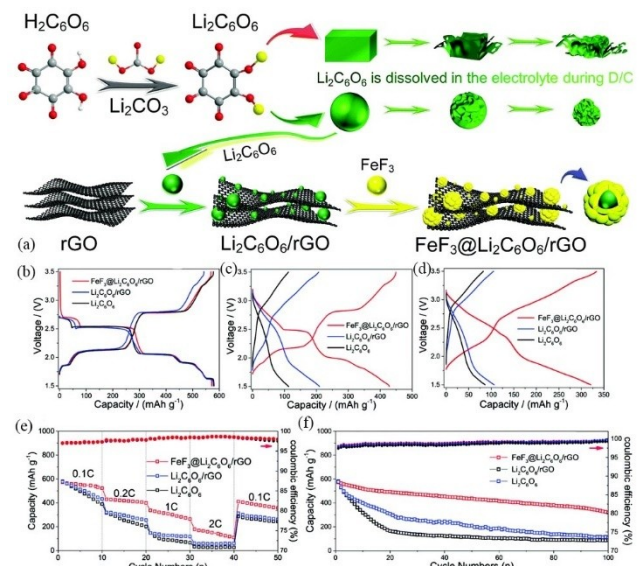


Figure 5. a) Schematic diagram of $\text{Li}_2\text{C}_6\text{O}_6$ with different morphologies and simulation diagram of the process of extraction-insertion of lithium; b-d) charge/discharge curves of $\text{Li}_2\text{C}_6\text{O}_6$, $\text{Li}_2\text{C}_6\text{O}_6/\text{rGO}$ and $\text{FeF}_3@\text{Li}_2\text{C}_6\text{O}_6/\text{rGO}$ at 1st, 50th and 100th cycles, respectively; e) rate performance and coulombic efficiency of three samples at different rate and f) cycling life and coulombic efficiency of $\text{Li}_2\text{C}_6\text{O}_6$, $\text{Li}_2\text{C}_6\text{O}_6/\text{rGO}$ and $\text{FeF}_3@\text{Li}_2\text{C}_6\text{O}_6/\text{rGO}$ at 0.1 C. Reproduced from Ref. [37] with permission. Copyright (2018), Royal Society of Chemistry.

de/lithiation process, the bonding force weaken between C_6O_6 layers, which promoting the exfoliation of C_6O_6 layers and pulverization of $Li_2C_6O_6$.^[41] It was also evident from these figures that the FeF_3 coating could effectively slow down this phenomenon. Further, cycling and rate performance of $FeF_3@Li_2C_6O_6/rGO$ are significantly superior to $Li_2C_6O_6$ and $Li_2C_6O_6/rGO$ (Figure 5e,f). During the first cycle, spherical $Li_2C_6O_6$, $Li_2C_6O_6/rGO$ and $FeF_3@Li_2C_6O_6/rGO$ delivered a reversible capacity of about 590 mAh g^{-1} . On the one hand, due to the dissolution of the material in the electrolyte, spherical $Li_2C_6O_6$, $Li_2C_6O_6/rGO$ could only keep a specific capacity of about 100 mAh g^{-1} after 100 cycles at 0.1 C . On the other hand, $FeF_3@Li_2C_6O_6/rGO$ could retain a high capacity of about 320 mAh g^{-1} at the end of 100 cycles because of the protection provided by the FeF_3 layer along with the synergistic effect of rGO.^[37]

4.2. Anode Materials

Generally, oxocarbon based compounds have multiple redox sites, which provide high theoretical capacity thus become the potential anode materials for LIBs applications.^[16,19,36]

To overcome the problems of poor conductivity and high solubility in electrolytes of small organic molecules, Zhao *et al.* developed a grafting method. They successfully synthesized a composite material, tetrahydroxybenzoquinone-graphene oxide (THBQ-GO), which contained abundant active radical with conducting graphene framework (Figure 6a).^[36] As seen in Figure 6(a), THBQ molecules could form ester bonds through the esterification process, which could effectively inhibit the dissolution of THBQ in the electrolyte and even accelerate the electron transport. Further, graphene sheets with excellent electronic conductivity would serve as a continuous electron transport pathway for THBQ to improve the electrochemical performance.^[36] Surprisingly, THBQ-GO-2 (the mass ratio of THBQ and GO is 1:1) could deliver an ultrahigh reversible capacity of 1075.9 mAh g^{-1} at 50 mA g^{-1} , which is more than three times the capacity value of pure THBQ and GO electrodes (Figure 6b). Further, it could maintain 57.4% capacity after 2000 cycles at a high current density of 1000 mA g^{-1} (Figure 6c). Such excellent rate performance is due to its high electronic conductivity, fast ion transmission rate, and pseudo-capacitance behaviour (Figure 6d).^[36]

5. Oxocarbon Based Compounds for SIBs

As we know, sodium resources are abundant (compared with lithium) which is the most attractive feature of SIBs to replace LIBs.^[14b,42–44] Among different electrode materials for SIBs, oxocarbon based compounds have attracted considerable attentions owing to their high theoretical capacity.^[17a,19,26a,33b]

Other common advantages of sodium-based oxocarbon compounds are 1) it can be obtained directly from natural biomass (e.g., rhodizonic acid precursor can directly be separated from myo-inositol.), 2) simple to prepare (e.g., oxcarbons were

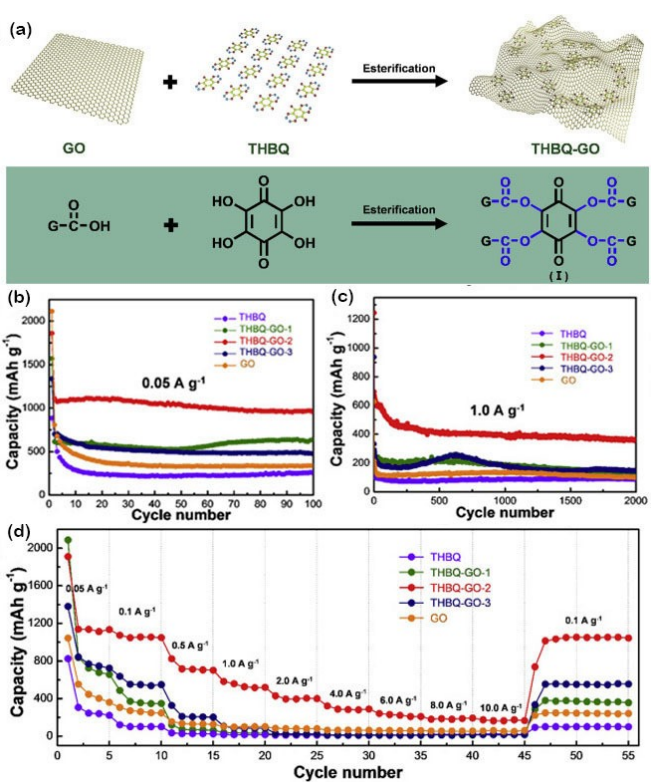


Figure 6. a) Schematic illustration of the formation of THBQ-GO composite; b) discharge specific capacity at 0.05 A g^{-1} ; c) capacity retention at 1.0 A g^{-1} ; and d) rate performance of different THBQ samples. Reproduced from Ref. [36] with permission. Copyright (2019), Elsevier.

prepared by proton exchange reactions,^[18] and 3) environmentally benign nature.^[18,19] In addition, oxocarbon based sodium salts (as a sodium host material) can form polar O–Na bonds during sodiation which can effectively alleviate the dissolution phenomenon of this organic compound in the electrolyte.^[14a]

Since Na^+ has a larger radius than Li^+ , many host materials suitable for lithium are not suitable for sodium.^[45] Although the oxocarbon based sodium salts mentioned in the discussion can be used as a host material for SIBs, these materials show poor conductivity, thus require a large amount of conductive agent. The conductive agent accounts for a large mass ratio in the prepared electrode, resulting in significant reduction in energy density and tap density of the cell.^[17a,27,46] In addition, although the dissolution in the electrolyte can be effectively alleviated by nanostructuring and adjusting the viscosity of the electrolyte, the dramatic degradation of the capacity upon cycling is still a big issue.^[19,26a] So far, the causes of the capacity attenuation are not clear. Finally, the safety performance of SIBs is still a problem which we need to solve prior to any practical application.^[42b,47]

5.1. Cathode Materials

The cathode material is the key to increase the capacity of SIBs. Numerous studies have focused on the development and

modification of cathode materials.^[16,27,41,48] Since 2008, when researchers firstly used $\text{Li}_2\text{C}_6\text{O}_6$ as a cathode material for LIBs, more and more research has been conducted on oxocarbon based sodium salts.^[15a] Due to the 25.5% larger diameter of Na^+ (1.02 Å) than Li^+ (0.76 Å),^[14a,49] material pulverization and crystal structure collapse could happen in electrodes during the process of sodiation/desodiation.^[49a,50] Thus, only a few oxocarbon materials have been investigated as active materials for SIBs.^[17a,22,26b] Nonetheless, $\text{Na}_2\text{C}_6\text{O}_6$ has become one of the favorable organic materials by scientists because of its unique layered structure and suitable metal ion (Li^+ and Na^+) intercalation/deintercalation mechanism.^[17b,19,33b] In 2013, Okada *et al.* reported $\text{Na}_2\text{C}_6\text{O}_6$ as cathode material for SIBs with a great reversible capacity of about 270 mAh g^{-1} , representing that each molecule could insert more than two sodium.^[17b] They also revealed that a high cut-off voltage could cause material dissolution into the organic electrolyte. While a low cut-off voltage would not cause any such dissolution, but it could cause peeling off of the electrode materials from the current collector. In the absence of a conducting agent, it could exhibit a repeated capacity of more than 90 mAh g^{-1} .^[17b] In fact, the energy density of $\text{Na}_2\text{C}_6\text{O}_6$ can be comparable to traditional inorganic materials of LIBs. However, its capacity tends to decay which hinders the practical applications.^[17b]

To study the electrochemical performance influencing factors of $\text{Na}_2\text{C}_6\text{O}_6$,^[26b] a research team explored the size effect of the material on electrochemical performance.^[26a] In this work, they prepared nanorod-shaped $\text{Na}_2\text{C}_6\text{O}_6$ which showed better sodium storage performance than microbulk and microrod structures (Figure 7a). The superior performance of nanorod-shaped $\text{Na}_2\text{C}_6\text{O}_6$ could be attributed to the smaller size of nanorods and the larger specific area (as compared to other shapes) which increase the contact area of the active material with the electrode solution thereby shortening the electron transmission distance and accelerating the ion transmission speed.^[26a] The electrochemical impedance spectroscopy (EIS) (Figure 7b) revealed that the interface impedance of $\text{Na}_2\text{C}_6\text{O}_6$ nanorods was much smaller and the ion diffusion efficiency was significantly higher than microbulk and microrod structures. As shown in Figure 7(c-f), during the charging process (desodiation), the XRD peaks shifted from 30.1° and 32.8° to 29.4° and 32.2°, respectively. The spacing between crystal planes changed upon charging, however, during discharge (sodium insertion) the XRD diffraction peaks returned to the original peak position, which could be the reason for its excellent cycle stability (it delivered a repeatable specific capacity about 190 mAh g^{-1} at a current rate of C/10 with over 90% retention after 100 cycles).^[26a] Although this material exhibits satisfactory electrochemical performance, its sodium storage mechanism is yet to be studied in a detailed manner. Cui and Bao *et al.* revealed that the reason for the limited electrochemical performance of $\text{Na}_2\text{C}_6\text{O}_6$ was due to the irreversible phase transition upon charge/discharge cycles.^[19] On the other hand, a study reported that 4 sodium ions could be stored, leading to an outstanding electrochemical performance (the repeatable capacity of 484 mAh g^{-1} , the largest energy density of approximately 726 Wh kg^{-1} and energy

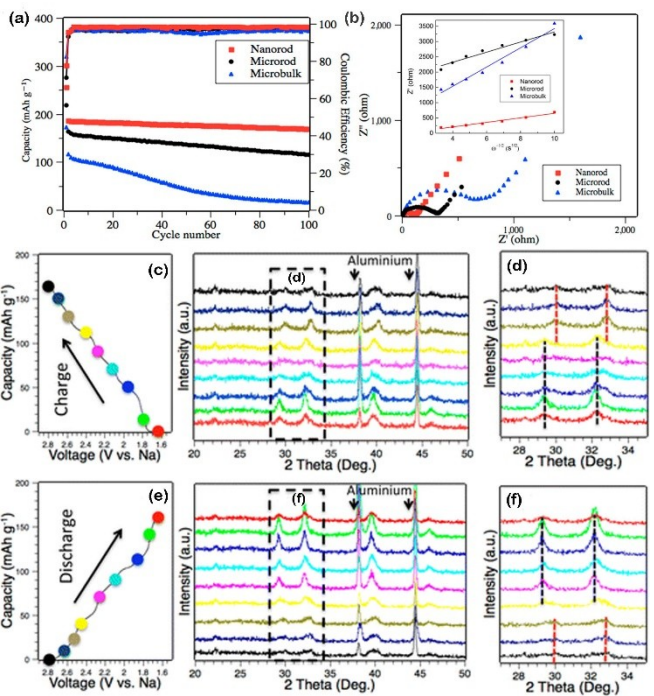


Figure 7. a) Capacity retention of $\text{Na}_2\text{C}_6\text{O}_6$ microbulk, microrod and nanorod; b) EIS spectra (the inset is real part of the complex impedance versus $\omega^{-1/2}$ at open circuit voltage); c) the charge curve of the $\text{Na}_2\text{C}_6\text{O}_6$ and the corresponding XRD patterns at different potential during the desodiation process. d) a magnified region of XRD diffraction patterns from 26° to 36° in c). e) the discharge curve of the $\text{Na}_2\text{C}_6\text{O}_6$ and the corresponding XRD patterns at different potential during the desodiation process. f) a magnified region of XRD diffraction patterns from 26° to 36° in e). Reproduced from Ref. [26a] with permission. Copyright (2016), American Chemical Society.

efficiency above 87%). This work proves that the organic electrode material can be a potential candidate for secondary battery application.^[19,51] In addition, studies have reported that the electrochemical performance can be enhanced through improving the conductivity of the material by different ways.^[17a,33b] For instance, Yuan *et al.* reported that $\text{Na}_2\text{C}_6\text{O}_6$ combined with conductive polyaniline (PANI) could be a potential cathode material for SIBs. This compound could form a good conducting network during the charging and discharging process. Further, they also reported that an appropriate composite approach could prevent the peeling off of the materials by decreasing the grain size.^[33b]

5.2. Anode Materials

In general, when oxocarbon based compounds are used as anode materials for SIBs, carbonyl groups (C=O) act as redox-active centers for charge/discharge cycles.^[14a] $\text{Na}_2\text{C}_6\text{O}_6$ was investigated as a cathode, while the $\text{Na}_2\text{C}_5\text{O}_5$ was explored as an anode material for SIBs at the same time. The $\text{Na}_2\text{C}_5\text{O}_5$ is a five-membered cyclic compound with three carbonyl groups. A study compared the properties of micro-sized $\text{Na}_2\text{C}_5\text{O}_5$ (CADS), submicro-sized $\text{Na}_2\text{C}_5\text{O}_5$ (sCADS), and graphene oxide wrapped $\text{Na}_2\text{C}_5\text{O}_5$ (GO-CADS). They proposed that the refined particles

could improve the reaction kinetics, and the substitution of graphene oxide could improve the conductivity. Further, it was revealed that the graphene oxide in the core-shell structure could improve the utilization rate of CADS.^[34] However, these materials showed dissolution in electrolyte, poor rate performance, and unstable cycling performance. To overcome these shortcomings, a research group constructed a novel three-dimensional (3D) architecture of $\text{Na}_4\text{C}_6\text{O}_6$ /graphene nanosheets via a simple hydrothermal method and further prepared a multi-level porous $\text{Na}_4\text{C}_6\text{O}_6$ -graphene- $\text{Na}_4\text{C}_6\text{O}_6$ sandwich structure. This unique porous structure greatly promoted the ion diffusion rate and electronic transmission speed. Further, the $\text{Na}_4\text{C}_6\text{O}_6$ /graphene structure showed low resistance and fast electron transfer rate. This composite structure could demonstrate an initial capacity of 885 mAh g^{-1} and a reversible capacity of 286 mAh g^{-1} after 90 cycles, exhibiting dramatic value. As shown in Figure 8, the 3D $\text{Na}_4\text{C}_6\text{O}_6$ -graphene structure could also provide good rate capability and long-term stability (capacity after 2000 cycles at 3720 mA g^{-1} was 80 mAh g^{-1}).^[20]

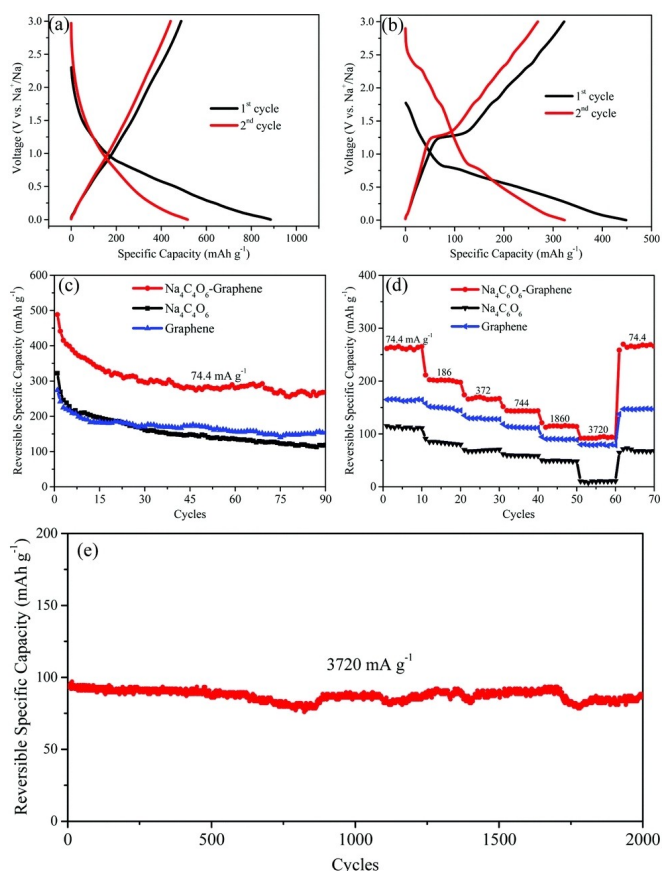


Figure 8. First two cycle charge-discharge studies of a) 3D $\text{Na}_4\text{C}_6\text{O}_6$ -graphene and b) $\text{Na}_4\text{C}_6\text{O}_6$; c,d) cycling and rate performance of graphene, pure $\text{Na}_4\text{C}_6\text{O}_6$ and 3D $\text{Na}_4\text{C}_6\text{O}_6$ -graphene; e) long cycling characteristics of 3D $\text{Na}_4\text{C}_6\text{O}_6$ -graphene at 3720 mA g^{-1} current density. Reproduced from Ref. [20] with permission. Copyright (2017), Royal Society of Chemistry.

6. Oxocarbon Based Compounds for PIBs

Potassium has abundant reserves in the earth's crust, which is ~ 1229 times of lithium resources. Hence, potassium based materials could meet the ever-growing energy demands. At the same time, it can be a potential candidate for large-scale and cost-effective energy storage applications.^[39b,52] K^+ possesses lower standard electrode potential than Li^+/Li , which allows a higher operating potential, thereby effectively increasing the energy density of the battery.^[53] Further, the weak solvation of K^+ in most of the electrolytes leads to an improved K^+ diffusion rate in potassium based electrodes.^[52b,53a,54] In addition, the potassium based compounds can be prepared easily and obtained directly from natural materials.^[18] Among different oxocarbons, $\text{K}_2\text{C}_6\text{O}_6$ shows superior electronic conductivity and possesses layered structure. Thus, K^+ can be easily diffused between these layers, and electrons can effectively move along the conjugated benzene ring layer.^[18]

The larger radius of K^+ will influence the reaction kinetics, electrochemical performance and even destroy the structure of the materials upon redox processes as compared to Li^+ .^[39b,55] Another drawback is the high solubility of oxocarbon based compounds in aprotic electrolytes, leading to poor cycling performance.^[17b,34] Similar to most of the organic anode materials, oxocarbon based anode materials have low electronic conductivity.^[12a,27,33b] In addition, the formation of potassium dendrites could be a threat to battery safety. Also it will lead to poor Coulombic efficiency as well as low cycle life.^[54c]

6.1. Cathode Materials

The radius of K^+ is much larger than Li^+ ,^[6d,7c,54a] therefore, we should select suitable electrode materials that allow rapid transport of potassium ions in the crystal lattice.^[56] Chen and collaborators explored oxocarbon based potassium salts ($\text{K}_2\text{C}_4\text{O}_4$, $\text{K}_2\text{C}_5\text{O}_5$, and $\text{K}_2\text{C}_6\text{O}_6$) as positive materials for PIBs.^[18] In this study, they found that $\text{K}_2\text{C}_4\text{O}_4$ had very less redox activity. Further, this study revealed that the five-membered ring ($\text{K}_2\text{C}_5\text{O}_5$) was the smallest ring that could insert K^+ , while $\text{K}_2\text{C}_6\text{O}_6$ could show excellent rate performance due to the larger ring size. By reducing the amount of conductive agent in the $\text{K}_2\text{C}_6\text{O}_6$ based electrode, it was found that the rate performance remained unchanged which could be attributed to its inherent properties.^[18] Studies have shown that the smaller Stoke's radius of solvated K^+ could be the reason for its higher diffusion rate and better rate capability.^[53a,54a,56] Further, many studies reported the high diffusion coefficient of K^+ , following in excellent rate performance of $\text{K}_2\text{C}_6\text{O}_6$.^[18] Figure 9(a,b) demonstrates the charge-discharge curve and the in-situ characterization, which comprehensively prove that the $\text{K}_2\text{C}_6\text{O}_6$ could reversibly insert and extract two-potassium. Figure 9(c) represents the most stable structure of $\text{K}_2\text{C}_6\text{O}_6$, which is considered to be the two-potassium intercalated state. Further, the HOMO state of $\text{C}_6\text{O}_6^{4-}$ ion has not changed, indicating that the compound is stable after gaining two electrons (Figure 9d).

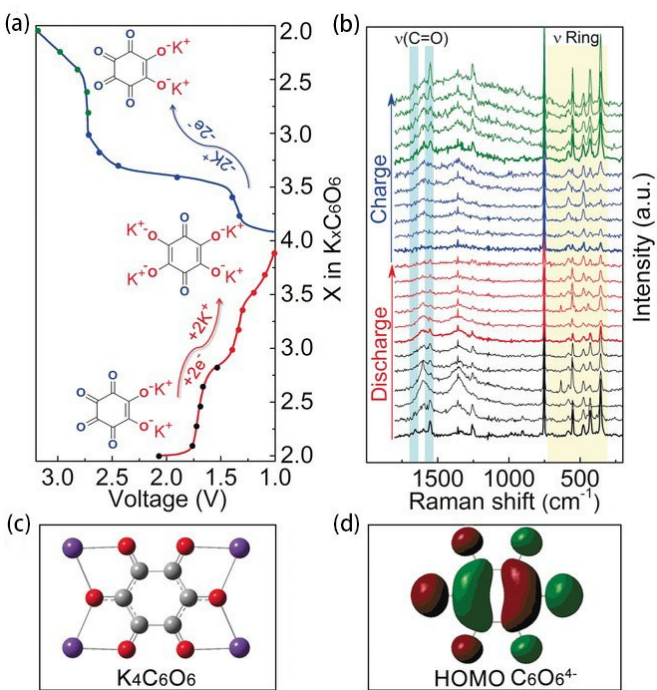


Figure 9. Reversible K^+ insertion/extraction of $\text{K}_2\text{C}_6\text{O}_6$. a) Charge/discharge curves with emphasis point for in-situ Raman test; b) corresponding Raman spectra; c) the most stable product structure in the discharge process (i.e. $\text{K}_4\text{C}_6\text{O}_6$); d) HOMO plots of $\text{C}_6\text{O}_6^{4-}$. Reproduced from Ref. [18] with permission. Copyright (2016), Wiley-VCH.

Chen *et al.* fabricated and evaluated an all-organic rocking-chair PIBs with $\text{K}_2\text{C}_6\text{O}_6$ as cathode and dipotassium terephthalate (K_2TP) as anode.^[57] The $\text{K}_2\text{C}_6\text{O}_6/\text{K}_2\text{TP}$ full-cell exhibited a high reversible capacity of 145 mAh g^{-1} with an average voltage of 1.5 V after 50 cycles and a moderate energy density of 52 Wh kg^{-1} . Although the electrochemical performance of the full-cell needs to be further improved, the use of oxocarbon salts as part of the all-organic battery seems to be promising.

6.2. Anode Materials

Due to the high activity of potassium metal, it is not considered as a superior candidate for the negative electrode applications. Researchers are still searching for suitable anode materials for PIBs.^[57,58] Oxocarbon salts were also explored as anode material for PIBs. Chen and co-workers assembled the first oxocarbon salt rocking-chair potassium ion full-cell with $\text{K}_2\text{C}_6\text{O}_6$ and $\text{K}_4\text{C}_6\text{O}_6$ as cathode and anode, respectively.^[18] This full-cell could demonstrate an average operating voltage of $\approx 1.1 \text{ V}$ and energy density of 35 Wh kg^{-1} . Although the performance of the full-cell is not ideal, the material is still expected to be widely used as a negative electrode for AIBs, owing to its high theoretical capacity, environmental friendliness, cost effectiveness and its unique layered structure. However, the larger ionic radius of K than Na and Li results in a severe structural deterioration in the process of taking off or embedding the potassium. Therefore, the selection of electrode materials will be more demanding for potassium ion batteries. At present,

the reported oxocarbons as negative electrode of potassium ion battery is still limited.

7. Challenges, Opportunities and Future Perspectives

High energy density, long cycle life, fast charge/discharge capability, low cost, and safety are the desirable properties of different AIBS applications.^[59] Oxocarbon compounds have attracted considerable attentions because of their unique properties. Identifying the challenges and opportunities of this category of materials are very important to design functional electrodes for different AIBs in the future.^[46,60]

7.1. Challenges

Although studies have reported the potential electrochemical performances, such as satisfactory rate performance, relatively high energy density, and ultrahigh capacity of oxocarbon compounds as electrode materials for AIBs,^[18] the related research is still in its infancy and needs to meet many challenges prior to any practical applications.

7.1.1. Poor Electronic Conductivity

The conductivity determines the rate capability of an electrode to a certain extent.^[13a,61] Mostly, oxocarbon compounds have non-metallic covalent bonds, and small amounts of ionic bonds, resulting in poor electronic conductivity. Due to its low electronic conductivity, the active material accounts for only a small proportion in the electrode, resulting in limited power and energy density in comparison to inorganic counterparts.^[13a,34]

7.1.2. Fast Capacity Decay

Oxocarbon compounds have been investigated as electrode materials for different AIBs, however, the huge capacity decay after the first cycle has been always a problem. The factors influencing this decay are as follows: a) high solubility of active material in organic electrolyte,^[15a,25,26b] b) volume expansion when cations are inserted into the oxocarbon compounds during charge/discharge cycles (particles pulverization trigger the peeling-off of the materials from the current collector),^[34] c) irreversible phase transition during the cycling,^[19] d) shuttle effect, uncontrollable organic redox intermediates consume alkali metal of anode.

7.2. Opportunities

7.2.1. Enhancing the Conductivity

The most direct way to increase the conductivity of an electrode is to add a conductive agent or graft it on the conducting material.^[33b,34,62] The addition of some conductive carbons (such as graphene and carbon nanotubes) can not only improve the conductivity of the electrode, but also produce a strong π - π bond interaction with oxocarbon compounds to prevent the dissolution of organic material into the electrolyte.^[36,63] Compositing the oxocarbons with the conductive polymer can make the pulverized active material not easily separated from the conductive polymer during the electrochemical cycle, thereby alleviating the capacity degradation.^[33b] Further, it reduces the high impedance caused by poor contact between the oxocarbon compounds and the current collector during the cycling process.^[33b]

7.2.2. Slowing Down Capacity Degradation

To improve the utilization rate of active materials and the electrochemical performances in the field of AlBs, the following strategies are proposed: a) controlling the nanoparticles granularity to improve the electrochemical performance of materials. Nano-sized materials have large specific surface area (resulting in effective utilization of active materials), and are more prone to chemical reactions (leading to enhanced reaction kinetics);^[19,27] b) electrolyte optimization. Reversible phase transition is a prerequisite for reversible intercalation/deintercalation of metal ions. Strongly solvation of diethylene glycol dimethyl ether (DEGDME) electrolyte can interfere between the anion and cation, which lower kinetic barrier of the phase transformation;^[19] c) selection of appropriate binders. Combining hydroxyl-rich binders with oxygen-rich active materials to generate self-healing hydrogen bonds is a common strategy to alleviate capacity degradation caused by material pulverization;^[26b,64] d) development a selective separator, metal-organic framework (MOF) gel membrane is a promising candidate because MOF has ideal ion and molecular sieving capability.^[65]

7.3. Future Perspectives

Although there are still many challenges associated with oxocarbon compounds, its excellent electrochemical properties (as shown in Table 1), wide range of resources and environmental benign nature make this category of materials the potential electrode active materials for different AlBs applications. For example, graphene grafted with organic molecules can exhibit a very high reproducible capacity of 1076 mAh g^{-1} .^[36] Numerous studies have shown that oxocarbons can become a superior electrode material with ultra-long cycle life, outstanding rate performance and ideal energy/power density for different energy storage applications.^[16] In addition, the continuous research and development of this material will help its promotion in the field of large-scale energy storage and portable electronic device applications.

8. Conclusions

In this review, from the perspective of electrochemical performance of oxocarbon compounds for different AlBs, we cover the evolution of oxocarbon compounds from four-membered to six-membered rings. As the electrode materials, people have reported that carbonyl groups are the redox active sites for oxocarbon based compounds. The active ingredient of the four-membered ring rechargeable battery has steric hindrance or electrostatic repulsion. The five-membered compound can reversibly insert/extract 2 metal ions. The six-membered ring can insert/extract 4 metal ions and has a higher operating voltage due to the lowest unoccupied molecular orbital (LUMO).^[18] Although certain materials show advantages as active materials, there are many challenges, such as low electronic conductivity and high solubility in organic electrolyte. Researchers have proposed many strategies to mitigate these challenges which includes nanostructuring, electrolyte/binder modifications and coating/grafting with conducting materials like carbon. As compared to inorganic materials, this type of material exhibits higher specific capacity, abundant resources, and green sustainability. From recent research, the strategy of preparing alkaline organic materials could promote the appropriate phase changes and overcome the dissolution

Table 1. Oxocarbon compounds for AlBs.

Type	Initial/reversible capacity [mAh g ⁻¹]	Average voltage [V]	Cycling life (capacity retention % cycle number)	Rate capability (capacity [mAh g ⁻¹] at current density [mA g ⁻¹])	Ref.
Cathode					
Li ₂ C ₆ O ₆	580	1.8, 2.5*	–	290 at 1.25 C	[15a]
Na ₂ C ₆ O ₆	498	1.5	90.6% (50)	371 at 1000	[19]
K ₂ C ₆ O ₆	212	2.4	66.7% (100)*	164 at 10 C	[18]
C ₆ O ₆	902	1.7	82% (100)	450 at 500	[16]
Anode					
Li ₄ C ₆ O ₆	223	1.8	90.5% (50)	223 at 1 C	[20]
Na ₂ C ₅ O ₅	293	1.7	50% (100)*	–	[25]
Na ₄ C ₆ O ₆	~270	1.25*	100% (60)	95 at 3720	[34]
H ₄ C ₆ O ₆	1075.9	1.65*	88.9% (100)	163.7 at 10000	[36]

*The data were calculated according to the graph.

through controlling particle size of nanoparticle and selection of suitable electrolyte.^[19] We believe that a series of strategies could contribute to the development of more inexpensive, efficient, and environmentally sustainable oxocarbon based compounds for different rechargeable batteries.

Acknowledgements

This work was financially supported by the National Nature Science Foundation of China (No. 21975289, No. 21905306 and No. U19A2019), Postdoctoral International Exchange Program Funding of China (No. 115) and China Postdoctoral Science Foundation (No. 2019M652802). This work was also financially supported by the Key R&D Project funded by Department of Science and Technology of Jiangsu Province (BE2020003), and the Opening Project of Material Corrosion and Protection Key Laboratory of Sichuan Province of China (No. 2020CL11).

Conflict of Interest

The authors declare no conflict of interest.

Keywords: alkali ion batteries • electrochemical performance • electrochemical storage • organic materials • oxocarbons materials

- [1] a) K. Zou, P. Cai, Y. Tian, J. Li, C. Liu, G. Zou, H. Hou, X. Ji, *Small Methods* **2020**, *4*, 1900763; b) X. Zhou, Q. Liu, C. Jiang, B. Ji, X. Ji, Y. Tang, H. M. Cheng, *Angew. Chem. Int. Ed.* **2020**, *59*, 3802–3832; c) H. Jia, Z. Wang, B. Tawiah, Y. Wang, C.-Y. Chan, B. Fei, F. Pan, *Nano Energy* **2020**, *70*, 104523; d) S. Wu, Q. Zhang, D. Sun, J. Luan, H. Shi, S. Hu, Y. Tang, H. Wang, *Chem. Eng. J.* **2020**, *383*, 123162; e) J. Wang, J. G. Wang, H. Liu, Z. You, Z. Li, F. Kang, B. Wei, *Adv. Funct. Mater.* **2020**, *31*, 2007397; f) Q. Zhang, J. Luan, L. Fu, S. Wu, Y. Tang, X. Ji, H. Wang, *Angew. Chem. Int. Ed.* **2019**, *58*, 15841–15847; g) Y. Zhang, B. Zhang, J. Li, J. Liu, X. Huo, F. Kang, *Chem. Eng. J.* **2021**, *403*, 126377; h) H. Jiao, S. Jiao, S. Li, W.-L. Song, H. Chen, J. Tu, M. Wang, D. Tian, D. Fang, *Chem. Eng. J.* **2020**, *391*, 123594; i) K. V. Kravchyk, M. V. Kovalenko, *Adv. Energy Mater.* **2020**, *10*, 2002151.
- [2] a) Q. Zhao, W. Huang, Z. Luo, L. Liu, Y. Lu, Y. Li, L. Li, J. Hu, H. Ma, J. Chen, *Sci. Adv.* **2018**, *4*, eaao1761; b) W. Guo, S. Shu, T. Zhang, Y. Jian, X. Liu, *ACS Appl. Mater. Interfaces* **2020**, *3*, 2983–2988; c) M. Di, L. Hu, L. Gao, X. Yan, W. Zheng, Y. Dai, X. Jiang, X. Wu, G. He, *Chem. Eng. J.* **2020**, *399*, 125833; d) X. Zhao, V. P. Lehto, *Nanotechnology* **2021**, *32*, 042002; e) T.-F. Yi, T.-T. Wei, Y. Li, Y.-B. He, Z.-B. Wang, *Energy Storage Mater.* **2020**, *26*, 165–197; f) H. Li, M. Xu, C. Gao, W. Zhang, Z. Zhang, Y. Lai, L. Jiao, *Energy Storage Mater.* **2020**, *26*, 325–333; g) Y. Nie, W. Xiao, C. Miao, M. Xu, C. Wang, *Electrochim. Acta* **2020**, *334*, 135654; h) H. He, D. Sun, Y. Tang, H. Wang, M. Shao, *Energy Storage Mater.* **2019**, *23*, 233–251.
- [3] X. Zhao, Z. Zhao-Karger, M. Fichtner, X. Shen, *Angew. Chem. Int. Ed.* **2020**, *59*, 5902–5949.
- [4] a) D. Sehrawat, J. Zhang, D. Y. W. Yu, N. Sharma, *Small Methods* **2018**, *3*; b) J.-N. Zhang, Q. Li, C. Ouyang, X. Yu, M. Ge, X. Huang, E. Hu, C. Ma, S. Li, R. Xiao, W. Yang, Y. Chu, Y. Liu, H. Yu, X.-Q. Yang, X. Huang, L. Chen, H. Li, *Nat. Energy* **2019**, *4*, 594–603; c) X. Sun, K. Tan, Y. Liu, J. Zhang, L. Hou, C. Yuan, *Chin. Chem. Lett.* **2020**, *31*, 2254–2258.
- [5] a) L. Chen, Z. Zhong, S. Ren, D.-M. Han, *Energy Technol.* **2020**, *8*; b) R. Rajagopalan, Z. Zhang, Y. Tang, C. Jia, X. Ji, H. Wang, *Energy Storage Mater.* **2021**, *34*, 171–193; c) M. Kim, M. Avdeev, B. Kang, *ACS Energy Lett.* **2019**, *5*, 403–410.
- [6] a) J. Nai, X. W. D. Lou, *Adv. Mater.* **2019**, *31*, e1706825; b) Q. Yang, F. Mo, Z. Liu, L. Ma, X. Li, D. Fang, S. Chen, S. Zhang, C. Zhi, *Adv. Mater.* **2019**, *31*, e1901521; c) W. J. Li, C. Han, G. Cheng, S. L. Chou, H. K. Liu, S. X. Dou, *Small* **2019**, *15*, e1900470; d) C. Zhang, Y. Xu, M. Zhou, L. Liang, H. Dong, M. Wu, Y. Yang, Y. Lei, *Adv. Funct. Mater.* **2017**, *27*, 1604307.
- [7] a) N. Zhang, F. Cheng, J. Liu, L. Wang, X. Long, X. Liu, F. Li, J. Chen, *Nat. Commun.* **2017**, *8*, 405; b) H. Li, X. Yu, Y. Bai, F. Wu, C. Wu, L.-Y. Liu, X.-Q. Yang, *J. Mater. Chem. A* **2015**, *3*, 9578–9586; c) J. Chu, W. A. Wang, J. Feng, C. Y. Lao, K. Xi, L. Xing, K. Han, Q. Li, L. Song, P. Li, X. Li, Y. Bao, *ACS Nano* **2019**, *13*, 6906–6916.
- [8] a) C. Zhao, Z. Chen, W. Wang, P. Xiong, B. Li, M. Li, J. Yang, Y. Xu, *Angew. Chem. Int. Ed.* **2020**, *59*, 11992; b) B. Wang, T. Ruan, Y. Chen, F. Jin, L. Peng, Y. Zhou, D. Wang, S. Dou, *Energy Storage Mater.* **2020**, *24*, 22–51; c) Z. Yan, Q.-W. Yang, Q. Wang, J. Ma, *Chin. Chem. Lett.* **2020**, *31*, 583–588.
- [9] a) C. Liu, Z. Neale, J. Zheng, X. Jia, J. Huang, M. Yan, M. Tian, M. Wang, J. Yang, G. Cao, *Energy Environ. Sci.* **2019**, *12*, 2273–2285; b) W. Yang, J. Zhou, S. Wang, W. Zhang, Z. Wang, F. Lv, K. Wang, Q. Sun, S. Guo, *Energy Environ. Sci.* **2019**, *12*, 1605–1612; c) G. Fang, C. Zhu, M. Chen, J. Zhou, B. Tang, X. Cao, X. Zheng, A. Pan, S. Liang, *Adv. Funct. Mater.* **2019**, *29*, 1808375.
- [10] a) Q. Zhang, J. Mao, W. K. Pang, T. Zheng, V. Sencadas, Y. Chen, Y. Liu, Z. Guo, *Adv. Energy Mater.* **2018**, *8*, 1703288; b) W. Zhou, H. Xie, S. Wang, Q. Wang, P. Jena, *Carbon* **2020**, *168*, 163–168.
- [11] a) H. Zhang, H. He, J. Luan, X. Huang, Y. Tang, H. Wang, *J. Mater. Chem. A* **2018**, *6*, 23318–23325; b) T. H. Kim, C. M. Park, *Batteries & Supercaps* **2020**, *4*, 112–119; c) X. Chen, C. Cheng, M. Ding, Y. Xia, L. Y. Chang, T. S. Chan, H. Tang, N. Zhang, L. Zhang, *ACS Appl. Mater. Interfaces* **2020**, *12*, 43665–43673; d) J. Zhang, Z. Cao, L. Zhou, G. Liu, G.-T. Park, L. Cavallo, L. Wang, H. N. Alshareef, Y.-K. Sun, J. Ming, *ACS Energy Lett.* **2020**, *5*, 2651–2661; e) Y. Zhao, L. Yang, C. Ma, G. Han, *Energy Fuels* **2020**, *34*, 8993–9001.
- [12] a) R. Rajagopalan, Y. Tang, X. Ji, C. Jia, H. Wang, *Adv. Funct. Mater.* **2020**, *30*, 1909486; b) D. Sun, D. Ye, P. Liu, Y. Tang, J. Guo, L. Wang, H. Wang, *Adv. Energy Mater.* **2018**, *8*, 1702383.
- [13] a) Y. Lu, J. Chen, *Nat. Chem. Rev.* **2020**, *4*, 127–142; b) T. Sun, J. Xie, W. Guo, D. S. Li, Q. Zhang, *Adv. Energy Mater.* **2020**, *10*, 1904199.
- [14] a) R. Rajagopalan, Y. Tang, C. Jia, X. Ji, H. Wang, *Energy Environ. Sci.* **2020**, *13*, 1568; b) Q. Zhao, Y. Lu, J. Chen, *Adv. Energy Mater.* **2017**, *7*, 1601792.
- [15] a) H. Chen, M. Armand, G. Demaillly, F. Dolhem, P. Poizot, J. M. Tarascon, *ChemSusChem* **2008**, *1*, 348–355; b) Y. Hu, W. Tang, Q. Yu, X. Wang, W. Liu, J. Hu, C. Fan, *Adv. Funct. Mater.* **2020**, *30*, 2000675; c) H. Wang, P. Hu, J. Yang, G. Gong, L. Guo, X. Chen, *Adv. Mater.* **2015**, *27*, 2348–2354.
- [16] Y. Lu, X. Hou, L. Miao, L. Li, R. Shi, L. Liu, J. Chen, *Angew. Chem. Int. Ed.* **2019**, *58*, 7020–7024.
- [17] a) X. Wang, P. Zhang, X. Tang, J. Guan, X. Lin, Y. Wang, X. Dong, B. Yue, J. Yan, K. Li, H. Zheng, H.-k. Mao, *J. Phys. Chem. C* **2019**, *123*, 17163–17169; b) K. Chihara, N. Chujo, A. Kitajou, S. Okada, *Electrochim. Acta* **2013**, *110*, 240–246.
- [18] Q. Zhao, J. Wang, Y. Lu, Y. Li, G. Liang, J. Chen, *Angew. Chem. Int. Ed.* **2016**, *55*, 12528–12532.
- [19] M. Lee, J. Hong, J. Lopez, Y. Sun, D. Feng, K. Lim, W. C. Chueh, M. F. Toney, Y. Cui, Z. Bao, *Nat. Energy* **2017**, *2*, 861–868.
- [20] J. Gu, Y. Gu, S. Yang, *Chem. Commun.* **2017**, *53*, 12642–12645.
- [21] S. Cohen, J. R. Lacher, J. D. Park, *J. Am. Chem. Soc.* **1959**, *81*, 3480–3480.
- [22] T. Yamashita, H. Momida, T. Oguchi, *Electrochim. Acta* **2016**, *195*, 1–8.
- [23] T. Yamashita, H. Momida, T. Oguchi, *J. Phys. Soc. Jpn.* **2015**, *84*, 074703.
- [24] M. Yi, L. Yang, J. Ma, H. Liu, M. He, C. Hu, P. Yu, *Biochem. Eng. J.* **2020**, *164*, 107792.
- [25] H. Chen, M. Armand, M. Courty, M. Jiang, C. P. Grey, F. Dolhem, J. M. Tarascon, P. Poizot, *J. Am. Chem. Soc.* **2009**, *131*, 8984–8988.
- [26] a) Y. Wang, Y. Ding, L. Pan, Y. Shi, Z. Yue, Y. Shi, G. Yu, *Nano Lett.* **2016**, *16*, 3329–3334; b) C. Wang, Y. Fang, Y. Xu, L. Liang, M. Zhou, H. Zhao, Y. Lei, *Adv. Funct. Mater.* **2016**, *26*, 1777–1786.
- [27] C. Luo, R. Huang, R. Kevorkyan, M. Pavanello, H. He, C. Wang, *Nano Lett.* **2014**, *14*, 1596–1602.
- [28] D. Braga, L. Maini, F. Grepioni, *Chem. Eur. J.* **2002**, *8*, 1804.
- [29] Q. Li, S. Li, K. Wang, W. Li, J. Liu, B. Liu, G. Zou, B. Zou, *J. Chem. Phys.* **2012**, *137*, 184905.
- [30] a) M. C. C. Ribeiro, A. O. Cavalcante, *Phys. Chem. Chem. Phys.* **2002**, *4*, 2917–2918; b) S. L. Georgopoulos, H. C. Garcia, H. G. M. Edwards, L. F. Capra de Oliveira, *J. Mol. Struct.* **2016**, *1108*, 542–551.
- [31] R. West, H.-Y. Niu, D. L. Powell, M. V. Evans, *J. Am. Chem. Soc.* **1960**, *82*, 6204–6205.

- [32] a) J. Tian, D. Cao, X. Zhou, J. Hu, M. Huang, C. Li, *ACS Nano* **2018**, *12*, 3424–3435; b) R. E. Dinnebier, H. Nuss, M. Jansen, *Acta Crystallogr. Sect. E* **2005**, *61*, m2148–m2150.
- [33] a) C. Frayret, E. I. Izgorodina, D. R. MacFarlane, A. Villesuzanne, A. L. Barres, O. Politano, D. Rebeix, P. Poizot, *Phys. Chem. Chem. Phys.* **2012**, *14*, 11398–11412; b) Y. Huang, G. Jiang, J. Xiong, C. Yang, Q. Ai, H. Wu, S. Yuan, *Appl. Surf. Sci.* **2020**, *499*, 143849.
- [34] C. Luo, Y. Zhu, Y. Xu, Y. Liu, T. Gao, J. Wang, C. Wang, *J. Power Sources* **2014**, *250*, 372–378.
- [35] a) J. Martínez De Ilarduya, L. Otaegui, M. Galcerán, L. Acebo, D. Shanmukaraj, T. Rojo, M. Armand, *Electrochim. Acta* **2019**, *321*, 134693; b) E. Marelli, C. Marino, C. Bolli, C. Villevieille, *J. Power Sources* **2020**, *450*, 227617.
- [36] Y. Wang, X. Li, L. Chen, Z. Xiong, J. Feng, L. Zhao, Z. Wang, Y. Zhao, *Carbon* **2019**, *155*, 445–452.
- [37] C. Lu, C. Dong, H. Wu, D. Ni, W. Sun, Z. Wang, K. Sun, *Chem. Commun.* **2018**, *54*, 3235–3238.
- [38] Y. Na, X. Sun, A. Fan, S. Cai, C. Zheng, *Chin. Chem. Lett.* **2021**, *32*, 973–982.
- [39] a) J. Kim, S. Ko, C. Noh, H. Kim, S. Lee, D. Kim, H. Park, G. Kwon, G. Son, J. W. Ko, Y. Jung, D. Lee, C. B. Park, K. Kang, *Angew. Chem. Int. Ed.* **2019**, *58*, 16764–16769; b) X. Yang, R. Zhang, *J. Alloys Compd.* **2020**, *834*, 155191.
- [40] a) C. A. Hansen, A. B. Dean, K. M. Draths, J. W. Frost, *J. Am. Chem. Soc.* **1999**, *121*, 3799–3800; b) R. J. Wodzinski, A. H. J. Ullah, *Adv. Appl. Microbiol.* **1996**, *42*, 263–302.
- [41] H. Kim, D.-H. Seo, G. Yoon, W. A. Goddard, Y. S. Lee, W.-S. Yoon, K. Kang, *J. Phys. Chem. Lett.* **2014**, *5*, 3086–3092.
- [42] a) M. D. Slater, D. Kim, E. Lee, C. S. Johnson, *Adv. Funct. Mater.* **2013**, *23*, 947–958; b) X. Zheng, C. Bommier, W. Luo, L. Jiang, Y. Hao, Y. Huang, *Energy Storage Mater.* **2019**, *16*, 6–23.
- [43] H. G. Wang, X. B. Zhang, *Chemistry* **2018**, *24*, 18235–18245.
- [44] C. Xia, S. Zhu, M. Tang, S. Xu, Y. Wu, C. Jiang, Y. Chen, S. Zhuo, B. Wang, C. Wang, *J. Phys. Chem. C* **2018**, *122*, 21185–21191.
- [45] a) D. Sun, D. Huang, H. Y. Wang, G. L. Xu, X. Y. Zhang, R. Zhang, Y. G. Tang, D. Abd El-Hady, W. Alshitar, A. S. AL-Bogami, K. Amine, M. H. Shao, *Nano Energy* **2019**, *61*, 361–369; b) Y. Wu, S. Hu, R. Xu, J. Wang, Z. Peng, Q. Zhang, Y. Yu, *Nano Lett.* **2019**, *19*, 1351–1358.
- [46] T. Jin, Q. Han, L. Jiao, *Adv. Mater.* **2020**, *32*, e1806304.
- [47] Y. Pi, Z. Gan, Z. Li, Y. Ruan, C. Pei, H. Yu, K. Han, Y. Ge, Q. An, L. Mai, *Nanoscale* **2020**, *12*, 21165–21171.
- [48] a) J. Tian, X. Zhou, Q. Wu, C. Li, *Energy Storage Mater.* **2019**, *22*, 218–227; b) D.-H. Seo, H. Kim, H. Kang, *Energy Environ. Sci.* **2011**, *4*, 4938.
- [49] a) B. Kong, L. Zu, C. Peng, Y. Zhang, W. Zhang, J. Tang, C. Selomulya, L. Zhang, H. Chen, Y. Wang, Y. Liu, H. He, J. Wei, X. Lin, W. Luo, J. Yang, Z. Zhao, Y. Liu, J. Yang, D. Zhao, *J. Am. Chem. Soc.* **2016**, *138*, 16533–16541; b) H. Yang, R. Xu, Y. Yao, S. Ye, X. Zhou, Y. Yu, *Adv. Funct. Mater.* **2019**, *29*, 1809195.
- [50] a) W. Cao, E. Zhang, J. Wang, Z. Liu, J. Ge, X. Yu, H. Yang, B. Lu, *Electrochim. Acta* **2019**, *293*, 364–370; b) Y.-H. Zhu, Q. Zhang, X. Yang, E.-Y. Zhao, T. Sun, X.-B. Zhang, S. Wang, X.-Q. Yu, J.-M. Yan, Q. Jiang, *Chem* **2019**, *5*, 168–179.
- [51] a) C. Lu, Z. Li, Z. Xia, H. Ci, J. Cai, Y. Song, L. Yu, W. Yin, S. Dou, J. Sun, Z. Liu, *Nano Res.* **2019**, *12*, 3051–3058; b) M. Ruby Raj, R. V. Mangalaraja, D. Contreras, K. Varaprasad, M. V. Reddy, S. Adams, *ACS Appl. Mater. Interfaces* **2019**, *3*, 240–252; c) H. Lyu, C. J. Jafta, I. Popovs, H. M. Meyer, J. A. Hachtel, J. Huang, B. G. Sumpter, S. Dai, X.-G. Sun, *J. Mater. Chem. A* **2019**, *7*, 17888–17895.
- [52] a) P. Xiong, X. Zhao, Y. Xu, *ChemSusChem* **2018**, *11*, 202–208; b) Y. Qi, Y. Yang, Q. Hou, K. Zhang, H. Zhao, H. Su, L. Zhou, X. Liu, C. Shen, K. Xie, *Chin. Chem. Lett.* **2021**, *32*, 1117–1120.
- [53] a) S. Komaba, T. Hasegawa, M. Dahbi, K. Kubota, *Electrochim. Commun.* **2015**, *60*, 172–175; b) W. Qiu, H. Xiao, Y. Li, X. Lu, Y. Tong, *Small* **2019**, *15*, e1901285; c) J. Ding, H. Zhang, H. Zhou, J. Feng, X. Zheng, C. Zhong, E. Paek, W. Hu, D. Mitlin, *Adv. Mater.* **2019**, *31*, e1900429; d) B. Xu, S. Qi, F. Li, X. Peng, J. Cai, J. Liang, J. Ma, *Chin. Chem. Lett.* **2020**, *31*, 217–222.
- [54] a) M.-H. Li, S.-Y. Zhang, H.-Y. Lv, W.-J. Li, Z. Lu, C. Yang, G.-H. Zhong, *J. Phys. Chem. C* **2020**, *124*, 6964–6970; b) S. Liu, J. Mao, Q. Zhang, Z. Wang, W. K. Pang, L. Zhang, A. Du, V. Sencadas, W. Zhang, Z. Guo, *Angew. Chem. Int. Ed.* **2020**, *59*, 3638–3644; c) M. Tang, Y. Wu, Y. Chen, C. Jiang, S. Zhu, S. Zhuo, C. Wang, *J. Mater. Chem. A* **2019**, *7*, 486–492.
- [55] L. Fan, R. Ma, J. Wang, H. Yang, B. Lu, *Adv. Mater.* **2018**, *30*, e1805486.
- [56] C. D. Wessells, S. V. Peddada, R. A. Huggins, Y. Cui, *Nano Lett.* **2011**, *11*, 5421–5425.
- [57] K. Lei, F. Li, C. Mu, J. Wang, Q. Zhao, C. Chen, J. Chen, *Energy Environ. Sci.* **2017**, *10*, 552–557.
- [58] a) I. Sultana, M. M. Rahman, T. Ramireddy, Y. Chen, A. M. Glushenkov, *J. Mater. Chem. A* **2017**, *5*, 23506–23512; b) X. Wu, Y. Chen, Z. Xing, C. W. K. Lam, S. S. Pang, W. Zhang, Z. Ju, *Adv. Energy Mater.* **2019**, *9*, 1900343.
- [59] a) R. Kumar, S. Sahoo, E. Joanni, R. K. Singh, W. K. Tan, K. K. Kar, A. Matsuda, *Prog. Energy Combust. Sci.* **2019**, *75*, 100786; b) T. Kim, W. Song, D.-Y. Son, L. K. Ono, Y. Qi, *J. Mater. Chem. A* **2019**, *7*, 2942–2964; c) K. Wang, S. Pei, Z. He, L.-a. Huang, S. Zhu, J. Guo, H. Shao, J. Wang, *Chem. Eng. J.* **2019**, *356*, 272–281; d) B. Dunn, H. Kamath, J. M. Tarascon, *Science* **2011**, *334*, 928–935.
- [60] a) Y. Sun, S. Guo, H. Zhou, *Adv. Energy Mater.* **2018**, *9*, 1800212; b) M. Z. Chen, Q. N. Liu, Y. Y. Zhang, G. C. Xing, S. L. Chou, Y. X. Tang, *J. Mater. Chem. A* **2020**, *8*, 16061–16080; c) K. Chayambuka, G. Mulder, D. L. Danilov, P. H. L. Notten, *Adv. Energy Mater.* **2020**, *10*, 2001310; d) X. Yin, S. Sarkar, S. Shi, Q. A. Huang, H. Zhao, L. Yan, Y. Zhao, J. Zhang, *Adv. Funct. Mater.* **2020**, *834*, 155191.
- [61] Y. Sun, N. Liu, Y. Cui, *Nat. Energy* **2016**, *1*, 16071.
- [62] a) Z. Wang, S. Li, Y. Zhang, H. Xu, *Phys. Chem. Chem. Phys.* **2018**, *20*, 7447–7456; b) L. Zhu, Q. Zhang, D. Sun, Q. Wang, N. Weng, Y. Tang, H. Wang, *Mater. Chem. Front.* **2020**, *4*, 2932–2942.
- [63] J. J. Shea, C. Luo, *ACS Appl. Mater. Interfaces* **2020**, *12*, 5361–5380.
- [64] C. Luo, X. Fan, Z. Ma, T. Gao, C. Wang, *Chem* **2017**, *3*, 1050–1062.
- [65] S. Bai, B. Kim, C. Kim, O. Tamwattana, H. Park, J. Kim, D. Lee, K. Kang, *Nat. Nanotechnol.* **2021**, *16*, 77–84.

Manuscript received: July 2, 2021

Revised manuscript received: August 17, 2021

Accepted manuscript online: August 20, 2021

Version of record online: August 31, 2021